Research Article

Saiqa Andleeb*, Faiza Tariq, Areesha Muneer, Tooba Nazir, Beenish Shahid, Zahid Latif, Shahab Ahmed Abbasi, Ihsan ul Haq, Zahid Majeed*, Salah Ud-Din Khan, Shahab Ud-Din Khan, Taj Muhammad Khan, and Dunia A. Al Farraj

In vitro bactericidal, antidiabetic, cytotoxic, anticoagulant, and hemolytic effect of green-synthesized silver nanoparticles using *Allium sativum* clove extract incubated at various temperatures

https://doi.org/10.1515/gps-2020-0051
received March 15, 2020; accepted July 09, 2020

Abstract: The current research aimed to evaluate *in vitro* biological activities of green-synthesized silver nanoparticles using the *Allium sativum* clove extract. The stability of green-synthesized silver nanoparticles was evaluated via storage at 4°C, room temperature (37°C), and calcined at 300°C, 500°C, and 700°C. The antibacterial effect was evaluated using agar well, spread plate, biofilm reduction, and cell proliferation inhibition assays. The cytotoxic and antidiabetic effects were determined via brine shrimp lethality, protein kinase inhibition, and α-amylase inhibition assays. DPPH scavenging, iron-chelating, anticoagulant, and hemolytic effects were evaluated. The highest inhibition of *Klebsiella pneumoniae* was observed when freshly prepared, calcined (300°C), and stored nanoparticles (4°C and 37°C) were applied (9.66, 9.55, 7.33, and 6.65 mm) against freshly prepared and calcined at 700°C which showed the highest inhibition of *Pseudomonas aeruginosa* (8.55 and 7.66 mm). Cell viability assay, biofilm reduction assay, and spread plate method showed a significant antibacterial effect of freshly prepared silver nanoparticles. Freshly prepared and calcined nanoparticles at 300°C and 500°C possessed strong antioxidant and iron-chelating activity. Among all the synthesized silver nanoparticles, freshly prepared and calcined nanoparticles (300°C and 500°C) increases the prothrombin time. Silver nanoparticles possessed significant anticoagulant properties and less toxic at least concentration toward human RBCs. In brine shrimp lethality assay, freshly prepared nanoparticles showed a stronger toxic effect and caused high mortality of larvae. Protein kinase inhibition assay revealed that freshly prepared nanoparticles had the highest zone of inhibition (18.0 mm) at 50 µg/disc. Green-synthesized nanoparticles would be used as potential therapeutic agents to overcome both infectious and noninfectious diseases.

Keywords: antibacterial effect, antidiabetic effect, anticoagulant effect, silver nanoparticles, *Allium sativum*

*** Corresponding author: Saiqa Andleeb,** Department of Zoology, Microbial Biotechnology Laboratory, University of Azad Jammu and Kashmir, Muzaffarabad, 13100, Pakistan, e-mail: drsaiqa@ajku.edu.pk
*** Corresponding author: Zahid Majeed,** Department of Biotechnology, University of Azad Jammu and Kashmir, Muzaffarabad, 13100, Pakistan, e-mail: zahid.majeed@ajku.edu.pk
Faiza Tariq, Areesha Muneer, Tooba Nazir, Zahid Latif: Department of Zoology, Microbial Biotechnology Laboratory, University of Azad Jammu and Kashmir, Muzaffarabad, 13100, Pakistan
Beenish Shahid: Department of Zoology, Physiology Laboratory, University of Azad Jammu and Kashmir, Muzaffarabad, 13100, Pakistan
Shahab Ahmed Abbasi: Department of Physics, University of Azad Jammu and Kashmir, Muzaffarabad, 13100, Pakistan
Ihsan ul Haq: Department of Pharmaceutical Sciences, Quaid-i-Azam University, Islamabad, Pakistan
Salah Ud-Din Khan: Sustainable Energy Technologies (SET) Center, College of Engineering, King Saud University, PO-Box 800, Riyadh, 11421, Saudi Arabia
Shahab Ud-Din Khan: National Tokamak Fusion Program, P.O. Nilore, 44000, Islamabad, Pakistan
Taj Muhammad Khan: National Institute of Lasers and Optronics (NILOP), P.O. Nilore, 45650, Islamabad, Pakistan
Dunia A. Al Farraj: Department of Botany and Microbiology, College of Science, King Saud University, PO-Box 800, Riyadh, 11421, Saudi Arabia

1 Introduction

The World Health Organization reported that more than 80% of the population of the world uses traditional medicine as a drug for its major healthcare requirements. There is a long history of the usage of

Open Access. © 2020 Saiqa Andleeb *et al.*, published by De Gruyter. This work is licensed under the Creative Commons Attribution 4.0 International License.

herbal drugs in Asia that shows interactions with the environment. For the treatment of infectious as well as chronic diseases, traditional medicinal plants have been used [1]. The towering environmental issues had attracted the researchers toward the novel green production of nanoparticles using living systems such as plants, fungi, and bacteria [2]. Biological nanoparticles are synthesized both by microorganisms and plants. These green synthesized nanoparticles are much better than nanoparticles synthesized from chemical protocols [3]. The biological nanoparticles have fast, environmental-friendly, and low-cost production strategies, and are biocompatible. Moreover, plants and microbes themselves act as stabilizing agents due to the presence of capping and stabilizing agents in them [4].

Green-synthesized silver nanoparticles (AgNPs) are being used as antifungal, antibacterial [5], antiviral [6], anti-inflammatory, and antioxidant agents [7]. Green production of AgNPs using different extracts of florae including *Bauhinia variegata* [8], *Anthemis atropatana* [9], *Caesalpinia pulcherrima* [10], *Cassia fistula* [11], *Euphrasia officinalis* [12], *Glycyrrhiza uralensis* [13], *Indigofera tinctoria* [14], *Bergenia ciliata* [15], and *Ipomoea batatas* [16] have been successfully reported. Lateef et al. [17] stated that *Petiveria alliacea* leaf extract was used to synthesize AgNPs and act as an antibacterial, antifungal, and anticoagulant agent.

Garlic (*Allium sativum* L. family Liliaceae) has long been used in traditional folk medicines of Iran, Europe, Mexico, and some other cultures. It is also used as a spice and food additive [18]. Garlic reduces blood pressure and cholesterol, and it has been used to prevent and treat cardiovascular disease and acts as anticancer and antimicrobial agents [19,20]. It is also used against diabetes and many more disorders [21–23].

Based on the medicinal importance of *A. sativum*, the aim of the current research was to synthesize and to characterize the biogenic GAgNPs using *A. sativum* extract (Gaqu) and to investigate the bactericidal effect, antioxidant potential, antidiabetic, and hemolytic efficacy of biogenic-synthesized GAgNPs and Gaqu extracts. Hopefully, the GBAgNPs could be used as a potential antibacterial agent to solve the multidrug-resistant problems, used as an antioxidant agent to reduce the oxidative stress, as antidiabetic and anticoagulant agents to aid the cardiovascular- and diabetes-related diseases. The outcomes of the current research could be the forward step for the pharmaceutical industries to modify or make the therapeutic drugs based on green nanotechnology.

2 Materials and methods

2.1 Chemicals, reagents, and equipment

All chemicals and reagents obtained from Sigma-Aldrich (Germany), Merck (Germany), Sigma-Aldrich (Switerzland), and Oxoid (Manchester). Nutrient broth, nutrient agar, Mueller–Hinton agar, crystal violet, MTT and acetic acid, methanol (Sigma-Allorich), dimethyl sulfoxide (DMSO; Fisher Scientific), DPPH (Alfa Aesar), sodium chloride and calcium chloride ($CaCl_2$) (Sigma-Allorich), ferrous sulfate ($FeSO_4$) and ferrozine (BDH), prothrombin time test tubes (PT tubes; Xinle). Steam sterilizer (Autoclave), 37°C shaking incubator, laminar flow, water distillery, refrigerator, centrifuge, spectrophotometer, furnace, flasks (250–1,000), test tubes, measuring cylinder, Petri plates, micropipette, filter papers, incubator 37°C (MMM Group Medcenter Enrichtungen GmbH), analytical balance (SARTORIUS GMBM GOTTINGEN, Germany), UV-Vis spectrophotometer (Shimadzu, Japan), FTIR (SHIMADZU-8400S), boiling water bath, electric hot plate (Wise-stir), scanning electron microscope, electronic balance or digital weighing machine (Jeweler Precision Balance Model: DH-V600A), distillery plant, filter paper disc, gloves, airtight reagent bottles, stirrer, pipettes, millimeter ruler, pestle, and mortar were used.

2.2 Collection of medicinal plants

Garlic (*Allium sativum*) was purchased from the supermarket of Muzaffarabad, Azad Kashmir, Pakistan. The bulb of garlic was peeled and crushed with pestle and mortar into fine pieces. A bulb of *A. sativum* was used for the preparation of aqueous extract (Gaqu) via maceration and boiling [24]. Two grams of *A. sativum* cloves were crushed and boiled in 100 mL of distilled water up to 100°C after adding in it. After boiling, it was left to cool at room temperature and filtered through filtration by using Whatman filter paper No. 1. An aqueous extract of *A. sativum* (Gaqu) after filtration was collected and used for further investigation.

2.3 Green synthesis of nanoparticles

GAgNPs synthesis from the bulb of *Allium sativum* was carried out as follows: 5 mL of aqueous extract of *Allium sativum* was mixed with 20 mL of 1 mM silver nitrate salt solution. It was heated until the color has been altered from yellow to brown. The color alteration specified the preliminary formation of GAgNPs. To yield a deep brown color, the solution was left for 24 h. Centrifugation of the solution was carried out at 20,000 rpm for 30 min. GAgNPs were settled down at the end of the tube and collected after washing with distilled water three times. GAgNPs were dried at 37°C in an incubator for 2 h. After preparation, dried GAgNPs were stored at three different conditions for one month, at room temperature (RT: 22°C), at 37°C, and at 4°C, and were also calcined or thermally treated at 300°C, 500°C, and 700°C for 1 h to observe the biological efficiency and stability of GAgNPs.

2.4 Characterization of nanoparticles

The primary characterization of green-synthesized nanoparticles (GAgNPs) was carried out via a UV-Vis spectrophotometer (PerkinElmer, LAMBDA 950 spectrometer). The absorbance was recorded at 200 nm between 800 nm. The size and shape of the synthesized nanoparticles were identified by using a scanning electron microscope (SEM: Jeol JSM-6510LV). GAgNPs were also used for FTIR spectrometric analysis (PerkinElmer Spectrum 100 series).

2.5 Agar well diffusion assay

Antibacterial assay of the aqueous extract of garlic (Gaqu), freshly prepared silver nanoparticles (FGAgNPs), calcined, and stored silver nanoparticles (GAgNPs) was performed using agar well-diffusion procedure against 10 pathogenic bacteria [25]. *Escherichia coli* (a), *Staphylococcus epidermidis*, *Pseudomonas aeruginosa*, *Klebsiella pneumoniae*, *Staphylococcus aureus* (a), *Serratia marcescens*, *Streptococcus pyogenes*, (isolated from clinical samples of blood and pus), *Escherichia coli* (b), *Staphylococcus aureus* (b), and *Staphylococcus aureus* (c) (isolated from an infected urine sample), respectively, were used. Nutrient agar and nutrient broth media (Oxoid CMOO3 and CM1) were used in bacterial culturing. An overnight culture (10^7 CFU/mL) and freshly prepared nutrient agar medium were mixed at 45°C and poured into the uncontaminated Petri plates. To solidify the culture, Petri dishes were set aside at room temperature in the laminar flow. After solidification, 5-mm wells were made using a sterilized micropipette tip of 1 mL, and an uncontaminated needle was used to remove the agar plug. About 30 µL of each 30 mg/mL of extracts (FGAgNPs), calcined and stored silver nanoparticles (GAgNPs) (1 mM) $AgNO_3$, and negative control (DMSO) were poured into the prepared wells, and then, Petri dishes were incubated at 37°C for 24 h. The bacterial growth reduction was measured through the diameter of the zone of inhibition in millimeter (mm) after 24 h [26]. The diameter was obtained by measuring the clear zones (if greater than 5 mm) around each well by using scale [27]. The growth sensitivity tests expressed as 0 mm means insensitivity, 1–3 mm is low sensitivity, greater than >3–6 mm shows moderate sensitivity, and greater than >6–10 mm regards for high sensitivity.

2.6 Spread plate count technique

In the spread plate count, bacterial colonies were developed on Petri dishes, and then their number was calculated [28]. In this method, all microbes were treated with different samples of GAgNPs (30 mg/mL), Gaqu (30 mg/mL), chloramphenicol, and $AgNO_3$ for overnight at 37°C. A test tube having positive control (broth + bacteria) was also stored. After 24 h, spreading of treated pathogens over the solidified Mueller–Hinton agar (CM 0337) was done. Then, the plates were incubated at 37°C for overnight. The next day, the colonies were counted.

2.7 Antibiofilm assay

The biofilm inhibition effect was evaluated via crystal violet assay with small modifications [29]. Bacterial pathogens were cultured at 37°C overnight in the Borosilicate tubes (Minitek, USA) having 30 mg/mL concentration of each Gaqu and GAgNPs. Chloramphenicol and DMSO were used as positive and negative controls. Tubes were incubated for 15 min, and the broth medium was removed after incubation. Later, 125 µL of a 0.1% crystal violet was added (through which attached cells were stained) and incubated for 10–15 min at room temperature. After incubation, crystal violet was washed

out with water to remove the unattached dye and cells. After the staining of biofilm, 30% acetic acid was added to solubilize crystal violet and then kept at room temperature for 10–15 min. Through spectrophotometer, solubilized crystal violet was quantified at the wavelength of 550 nm. As a blank, 30% acetic acid in water was used.

2.8 MTT assay

To estimate the viability of the bacterial cells, MTT assay used [30]. For the MTT assay, 0.2 mg/mL MTT (Genebase, China) in DMSO was mixed and incubated for almost 1–4 h at room temperature. Bacterial cells (100 µL) were grown in the nutrient broth medium (3 mL) at 37°C for overnight. The next day, the overnight culture was grown in the freshly prepared nutrient broth medium (1 mL) at 37°C for almost 3 h followed by pouring 100 µL of each test sample. To begin the reduction reaction, 10 µL of MTT stock solution was added, and this mixture was incubated at 37°C for at least 2–4 h (without shaking). A tube cap should be opened. The formation of formazan crystals was confirmed by the purple color. Later, 500 µL of DMSO was added in the tubes to dissolve the crystals of formazan at room temperature. By using a spectrophotometer, the values of all the samples were calculated at 570 nm, and DMSO was taken as a control.

2.9 Anticoagulant assay

In vitro anticoagulant effects of *A. sativum* extract (Gaqu) and its green-synthesized nanoparticles (GAgNPs) were examined in the blood samples by measuring prothrombin time (PT) [31]. About 10 mL of the blood was drawn from healthy volunteers by making vein puncture using sterile syringes. Blood was collected in a PT tube containing 3.8% trisodium citrate solution to avoid the natural coagulation process. Immediately, centrifugation was carried out for 15 min at a rate of 3,000 rpm. After centrifugation, blood cells were discarded and the plasma was collected. Plasma was used for the PT examination. The sample of plasma was separated into 9 groups: Group I: negative control; Group II: *A. sativum* extract (Gaqu.); Group III: freshly prepared silver nanoparticles (FGAgNPs); Group IV: GAgNPs (at room temperature); Group V: GAgNPs (at 37°C); Group VI: GAgNPs (at 4°C); Group VII: GAgNPs (at 300°C); Group VIII: GAgNPs (at 500°C); Group IX: GAgNPs (at 700°C). The water bath was used for incubating the tubes with a mixture at 37°C. To analyze the clot for every 30 s, all the tubes were tilted at an angle of 45°. The clot formation time was measured by using stopwatch. This time is called PT. Tests were repeated 3 times, and the average time was calculated.

2.10 Hemolytic activity

The spectrophotometer method is used to do *in vitro* hemolytic assay [32]. 100 µL of the *A. sativum* extract (30 mg/mL) and its green-synthesized silver nanoparticles (GAgNPs) (30 mg/mL) were added into 500 µL of the blood cell suspension. The water bath was used for incubating the tubes with a mixture at 37°C for 30 min. After incubation, it was centrifuged at 1,500 rpm for 10 min. The supernatant containing free hemoglobin was measured at 540 nm utilizing a UV-Vis spectrophotometer. Each experiment was repeated three times at each concentration. The level of percentage hemolysis by the *A. sativum* extract and its green-synthesized GAgNPs were calculated by using the formula: $([A_c - A_s]/A_c) \times 100$.

2.11 DPPH radical scavenging assay

The antioxidant assay of the *A. sativum* extract (Gaqu) and its green-synthesized silver nanoparticles (GAgNPs) was estimated using the method stated by Brand-Williams et al. [33], which is based on scavenging activity of the DPPH (1,1-diphenyl-2-picrylhyorazyl) free radical. 0.5 mM DPPH radical solution was prepared by mixing DPPH in methanol and stored in dark for 30 min. For the preparation of reaction mixture, 100 µL of the *A. sativum* extract (Gaqu.), freshly prepared FGAgNPs, 1 month stored (at room temperature, at 37°C and 4°C), and calcined (300°C, 500°C and 700°C) GAgNPs was added into 300 µL of 0.5 mM DPPH radical solution. After this, 3 mL of methanol was added and left for 30 min. The color has been changed from deep violet to light violet. The change in color indicates antioxidant activity. DPPH is reduced when it is reacted with an antioxidant agent that gives hydrogen. Absorbance (Abs.) of the reaction mixture was measured utilizing a UV-Vis spectrophotometer at 517 nm. For the preparation of the control solution, methanol (3 mL) was dissolved in DPPH

radical solution (0.3 mL). The level of percentage inhibition by the extract and green-synthesized AgNPs was calculated according to the subsequent formula: % Inhibition = $A_c - A_s/A_c \times 100$.

2.12 Iron-chelating activity

The chelation of Fe^{2+} by *A. sativum* aqueous extract (Gaqu) and its green-synthesized silver nanoparticles (GAgNPs) was assessed by the method of Dinis et al. [34]. For the preparation of reaction mixture, 50 µL of the garlic extract (Gaqu.), freshly prepared, stored (at room temperature, at 37°C and 4°C), and calcined (300°C, 500°C, and 700°C) GAgNPs samples was mixed with 500 µL of $FeSO_4$ (2 mM) solution. The reaction was initiated by the addition of 500 µL of 0.25 mM solution of ferrozine in a reaction mixture. The mixture was left at room temperature for 10 min after vigorously shaken. The control solution was prepared by mixing (500 µL) $FeSO_4$ (2 mM), 0.25 mM ferrozine (500 µL), and 50 µL of distilled water. The absorbance (Abs) of the mixture was measured at 562 nm using a UV-Vis spectrophotometer. The percentage inhibition of ferrozine–Fe^{2+} composite formation was estimated by using the formula $[(A_o - A_s)/A_o] \times 100$, where A_o signifies the control's absorbance and A_s signifies absorbance of the test samples.

2.13 α-Amylase inhibition assay

The inhibition of α-amylase was carried out by the method described by Malik and Singh [35]. Briefly, the reaction was initiated by the addition of 490, 470, and 450 µL buffer to different volumes (10, 30, and 50 µL) of 30 mg/mL of garlic extract, synthesized silver nanoparticles, stored (at room temperature, at 37°C and 4°C), and calcined (300°C, 500°C and 700°C) GAgNPs samples, respectively, to make the total volume of 500 µL reaction solution. In the next step, 500 µL α-amylase was added, followed by the addition of 1,000 µL of starch to the reaction vessels. Then, the reaction vessels were incubated in a water bath for 5 min at 100°C. Next to this step, 500 µL of NaOH is added. The reaction was completed by the addition of 500 µL of DNS, and then, the reaction vessels were again incubated for 5 min by putting them in a beaker with hot water. The color change from yellow to orange indicated α-amylase inhibition activity. For the preparation of blank, 30 µL of garlic extract was added into 1,500 µL buffer, and all the steps were conducted in the same sequence as mentioned earlier except the addition of amylase and starch. The tubes were left to cool, and the absorbance was measured at 540 nm. The percentage inhibition of α-amylase was calculated as $[(A_o - A_i)/A_o] \times 100$, where A_o was the absorbance of the standard and A_i was the absorbance of the test samples.

2.14 Protein kinase inhibitor assay

Streptomyces strain was used in protein kinase inhibition assay according to the method designated by Fatima et al. [36] with slight modification. A complete experiment was done under sterile conditions. Incubated *Streptomyces* strain was inoculated in the Tryptone Soya broth poured into Petri plates where the experimental organisms were left to grow. Filter paper discs were placed on the prepared loan media surface and a lesser concentration of test samples (garlic extract, newly synthesized or freshly prepared, stored (at room temperature, at 37°C, and 4°C) and calcined (300°C, 500°C, and 700°C)) GAgNPs, and standard were poured onto that surface. Surfactin- and DMSO-infused discs were taken as positive and negative controls, respectively. The plates were then incubated for 24–36 h for target strain growth and development. The results were interpreted as a bald zone of inhibition around sample- and control-infused discs.

2.15 Brine shrimp toxicity assay

The assay mixture was performed according to the method described by Bibi et al. [37]. The larvae of Brine shrimp (*Artemia salina*) were hatched at 37°C temperature in a bipartitioned tank that was filled with artificial seawater. The temperature of incubation was retained between 21°C and 30°C. On the second day after hatching of larvae, the hatched mature nauplii were collected and distributed to the 96-well plate. The stock solutions of test samples of garlic extract, freshly prepared, stored (at room temperature, at 37°C and 4°C), and calcined (300°C, 500°C, and 700°C) GAgNPs samples (30 mg/mL of DMSO) were diluted with seawater to have the final concentrations of 200, 100, 50, and 25 µg/mL for the lethality test. Then, these diluted solutions were transferred into each well containing 20

nauplii and dried yeast, and the mortality rate of these larvae was then determined. The negative control group was regarded as to the wells containing nauplii and seawater without the test samples, and the positive controls contained doxorubicin (4 mg/mL) along with seawater and nauplii. The plate was placed at room temperature for 1 day under fluorescent light. The experiment was repeated thrice, and the number of dead nauplii was counted in each well. The mortality was determined as a percentage of the positive control, and the LD_{50} was then calculated.

2.16 Statistical analysis

Each experiment has been done in triplicate. By using an online calculator (http://easycalculation.com/statistics/standard-deviation.php), mean ± standard deviation from the recorded values was calculated.

3 Results and discussion

3.1 Preliminary synthesis and characterization of GAgNPs

In the current research, GAgNPs were efficiently produced using Gaqu and $AgNO_3$ where phytochemicals present in Gaqu acted as reducing and stabilizing agents. The preliminary synthesis of GAgNPs was confirmed by a color change from light yellow to light brown. Our results are agreed with the findings of Zia et al. [15] and Shankar et al. [38] who showed the synthesis of green AgNps via color alteration when plant extracts were mixed with $AgNO_3$. Rajeshkumar [39], Donda et al. [40], and Sharma et al. [41] indicated similar results that color change indicates the preliminary synthesis of nanoparticles. Sharma et al. illustrated that surface-active particles play an important role in the reduction and stabilization processes of silver nanoparticles [41]. Phytochemical constituents in the plant extract interact with silver ions due to electrostatic interactions and then reduce these ions, which leads to form GAgNps. Flavones, amides, carboxylic acid, aldehydes, ketones, terpenoids, quinines, and anthraquinones play a primary role in the production of nanoparticles [42,43].

The preliminary characterization of the synthesized freshly prepared (FGAgNPs), one-month stored (at 4°C in the fridge, at room temperature, and 37°C), and calcined (300°C, 500°C, and 700°C) silver nanoparticles was determined by using UV-Vis spectrophotometer. Absorption bands are formed according to the size, shape, and chemical constituents of the produced AgNps [44]. The maximum UV-Vis absorption spectra were recorded at 200–329 nm. According to the visual analysis of spectra, the maximum absorption peak appears at 295 nm for FGAgNPs, and the maximum absorption peak recorded for one-month stored (at 4°C, at room temperature, and 37°C) GAgNPs was at 293, 294, and 295 nm, respectively. On the other hand, calcined GAgNPs gave the highest absorption peak at 295 nm

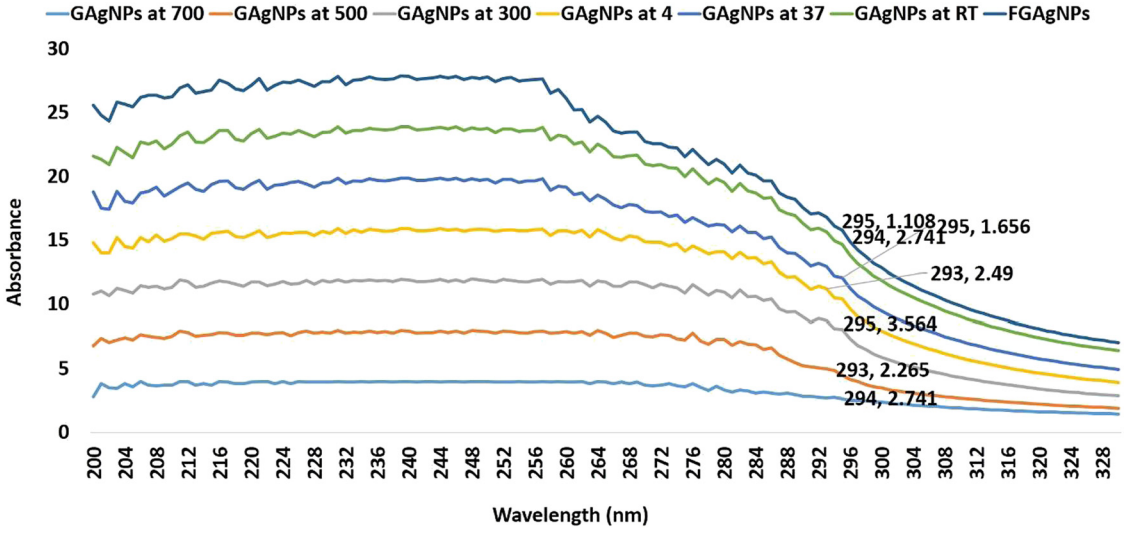

Figure 1: UV-Vis spectra analysis of green-synthesized silver nanoparticles using *A. sativum* clove extract.

(300°C), 293 nm (500°C), and 294 nm (700°C), respectively (Figure 1). Our findings correlate with El-Refai et al. [45]. They synthesized various metallic nanoparticles using garlic and ginger, and recorded a maximum absorption peak at 280 nm. It also depicts that the synthesis of Ag, Cu, Fe, and Zn nanoparticles was confirmed by analyzing the UV-Vis spectra. Otunola et al. [46] did UV-Vis absorption of AgNPs for garlic, and a clear peak was obtained at 375 nm. According to Ejaz et al. [47], it is concluded that AgNps produce the absorption band at around 200–800 nm in the UV-Vis spectra.

The size and morphology of fresh (FGAgNPs), stored, and calcined GAgNPs was analyzed by using scanning electron microscopy (Figure 2). The spherical shape of the synthesized GAgNPs was observed, and they were more aggregated. Their size ranged between 13.13 and 22.69 nm. Our result corresponded with the result of El-Refai et al. [45]. In another study, a spherical shape with 35 nm size of AgNPs synthesized by using *Bergenia ciliata* was observed by scanning electron microscopy [15].

Fourier Transform-Infrared Spectroscopy (FTIR) identifies molecular components and structures of sample by measuring the absorption of infrared radiation. Different peaks were appeared in fresh (FGAgNPs), stored, and calcined GagNps (Figure 3). Following strong peaks were obtained after FTIR analysis: The freshly synthesized (FGAgNps) had peaks at 498 nm (307 cm^{-1}), 493 nm (111 cm^{-1}), 487 nm (247 cm^{-1}), 480 nm (79 cm^{-1}), 465 nm (203 cm^{-1}), 448 nm (155 cm^{-1}), 434 nm (1,220 cm^{-1}), 429 nm (147 cm^{-1}), 417 nm (193 cm^{-1}), 408 nm (73 cm^{-1}). GAgNps stored at 4°C showed the peaks at 498 nm (301.4 cm^{-1}), 487 nm (281.0 cm^{-1}), 469 nm (276.8 cm^{-1}), 458 nm (79.6 cm^{-1}), 447 nm (169.4 cm^{-1}), 434 nm (1063.9 cm^{-1}), 429 nm (114.5 cm^{-1}), 425 nm (93.7 cm^{-1}), and 408 nm (65.2 cm^{-1}). Peaks of GAgNps stored at room temperature were 504 nm (169 cm^{-1}), 498 nm (172 cm^{-1}), 488 nm (248 cm^{-1}), 483 nm (187 cm^{-1}), 473 nm (117 cm^{-1}), 469 nm (316 cm^{-1}), 465 nm (50 cm^{-1}), 455 nm (237 cm^{-1}), 445 nm (58 cm^{-1}), 436 nm (61 cm^{-1}), 431 nm (663 cm^{-1}) 424 nm (102 cm^{-1}), 414 nm (254 cm^{-1}), and 405 nm (86 cm^{-1}). GAgNps stored at 37°C showed the following peaks: 498 nm (423 cm^{-1}), 487 nm (227 cm^{-1}), 470 nm (444 cm^{-1}), 458 nm (242 cm^{-1}), 447 nm (119 cm^{-1}), 434 nm (1,685 cm^{-1}), 427 nm (143 cm^{-1}), and 417 nm (178 cm^{-1}). GAgNps stored at 500°C had the following peaks: 524 nm (94 cm^{-1}), 514 nm (66 cm^{-1}), 498 nm (107 cm^{-1}), 489 nm (264 cm^{-1}), 469 nm (286 cm^{-1}), 458 nm (361 cm^{-1}), 444 nm (85 cm^{-1}), 434 nm (1255 cm^{-1}), 417 nm (153 cm^{-1}), and 408 nm (134 cm^{-1}). GAgNps stored at 300°C showed the following peaks: 527 nm (142.6 cm^{-1}), 515 nm (101.3 cm^{-1}), 505 nm (211.6 cm^{-1}), 498 nm (324 cm^{-1}), 487 nm (411 cm^{-1}), 483 nm (205.6 cm^{-1}), 480 nm (210.6 cm^{-1}), 470 nm (713.5 cm^{-1}), 465 nm (262.4 cm^{-1}), 458 nm (400.9 cm^{-1}), 447 nm (249.0 cm^{-1}), 434 nm (1470.4 cm^{-1}), 430 nm (184.3 cm^{-1}), and 416 nm (209.1 cm^{-1}). GAgNps stored at 700°C had the following peaks: 494 nm (408.91 cm^{-1}), 487 nm (445.55 cm^{-1}), 480 nm (235.38 cm^{-1}), 469 nm (745.57 cm^{-1}), 458 nm (296.37 cm^{-1}), 434 nm (2565.35 cm^{-1}), and 429 nm (132.42 cm^{-1}). All these peaks showed the presence of various functional groups in fresh, stored, and calcined GAgNps like 690–515 shows C–Br stretch that indicates the presence of alkyl halides;

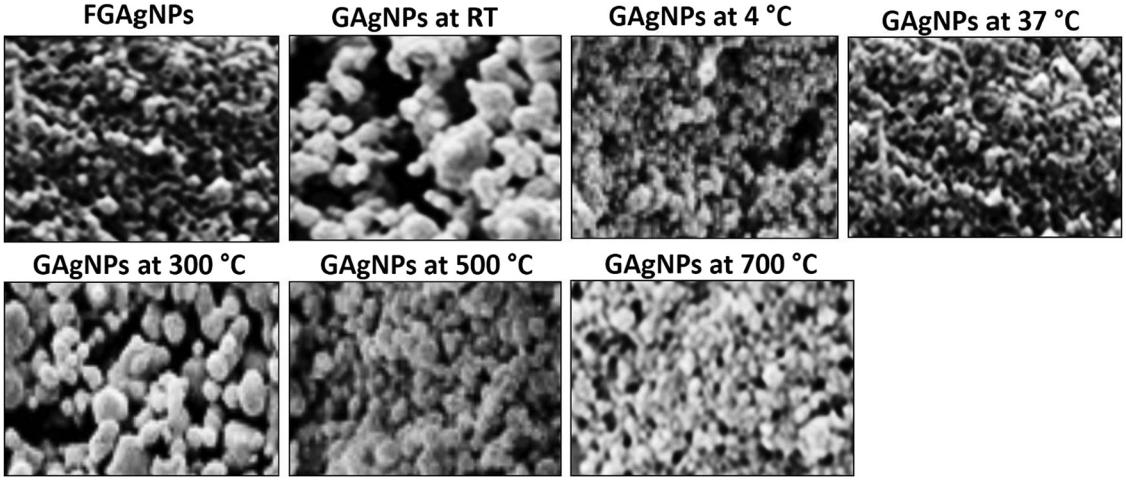

Figure 2: Scanning electron microscopy of synthesized silver nanoparticles using *A. sativum* clove extract.

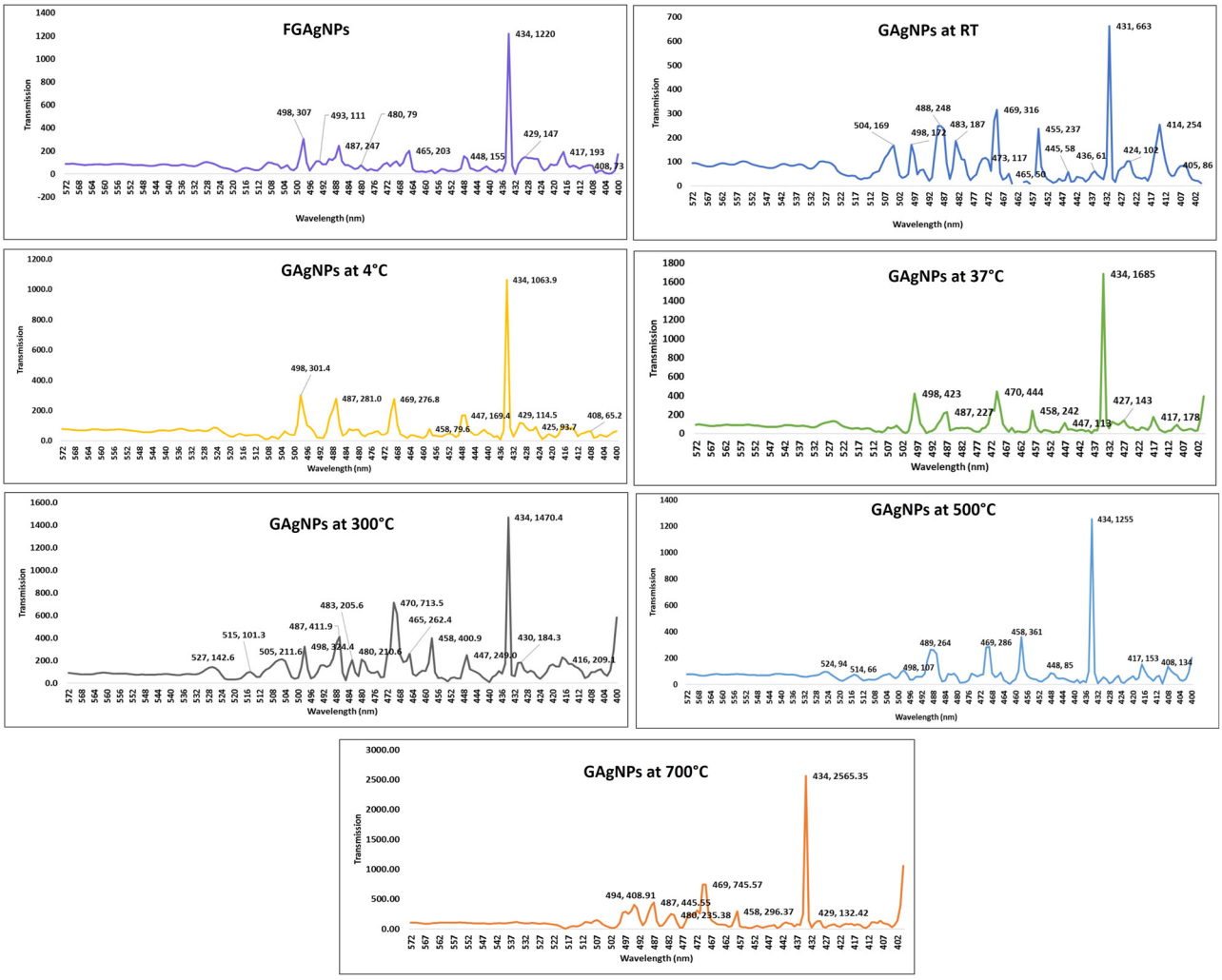

Figure 3: FTIR of green-synthesized silver nanoparticles using *A. sativum* clove extract.

852–550 m shows C–Cl stretch that indicates the presence of alkyl halides; 100–650 s shows C–H bond that indicates the presence of alkenes; 1,250–1,020 shows C–N stretch that indicates the presence of aliphatic amines; 1,300–1,100 shows C–O bond that indicates the presence of alcohols and carboxylic acid; 1,470–1,450 shows C–H bond that indicates the presence of alkanes; 1,710–1,665 shows C═O bond that indicates the presence of alpha-beta unsaturated aldehydes and ketones; 2,830–2,695 shows H–C═O:C–H bond that indicates the presence of aldehydes. Zia et al. [15] did FTIR of green-synthesized silver nanoparticles (BCAgNPs) using *Bergenia ciliata* and obtained peaks at 468.67, 609.46, 669.25, 1024.13, 1074.28, 1120.56, 1288.36, 1382.87, 2345.28, and 2368.42 cm^{-1}, which could be N–C═O amide, C–H stretch of aldehydes, C–H of alkanes, O–H of alcohol, N–H of amines, C═O of carboxylic acid/aldehydes or ester, H–C═O:C≡N stretch of nitriles. According to them, the shifts of functional groups indicate the participation of amide, hydroxyl, aldehydes, and carboxyl in the nanoparticle synthesis. The FTIR analysis by Otunola et al. [46] revealed different stretches of bonds at different peaks for each of the spices. The nanoparticles from garlic showed peaks at 1,048, 1,331, 1,583, 2,946, and at 3,317 characteristic of C–O (acid and ester stretch), C–N (amine), and O–H stretch/bends.

3.2 Antibacterial activity

The antibacterial activity of green-synthesized AgNps by the spread plate count and the agar well-diffusion method was evaluated, and our findings are agreed with the results of previous studies [15,47]. They showed that AgNps had a greater antibacterial effect compared to

Table 1: Antibacterial activity of green-synthesized silver nanoparticles (GAgNPs) and the extract of *Allium sativum* (Gaqu) against bacterial pathogens

Treatments	Bacterial pathogens									
	Serratia marcescens	***Streptococcus pyogenes***	***Klebsilla pneumonia***	***Staphylococcus aureus* (a)**	***Pseudomonas aeruginosa***	***Staphylococcus aureus* (b)**	***Staphylococcus aureus* (c)**	***Staphylococcus epidermidis***	***Escherichia coli* (a)**	***Escherichia coli* (b)**
Gaqu	4.0	7.0	5.66	6.33	5.66	0.33	2.0	0.33	4.33	1.66
FGAgNps	6.33	1.33	9.66	11.0	8. 33	1.33	7.0	1.33	5.33	5.0
4°C	1.0	2.0	7.33	6.33	6.66	4.33	5.0	4.33	0.67	4.66
RT	4.33	1.66	5.66	2.33	4.66	1.0	7.33	1.0	0.67	7.0
37°C	1.0	2.33	6.66	5.0	4.66	5.33	8.33	5.33	2.67	1.0
300°C	5.0	4.33	9.66	8.66	0.33	0.33	5.66	0.33	5.0	4.0
500°C	2.33	1.66	7.0	6.66	6.33	1.66	3.0	1.66	1.33	3.33
700°C	1.0	2.0	5.66	1.0	7.66	1.33	0.33	1.33	2.0	3.33

plant extract. According to Liao et al. [48], AgNPs have bactericidal roles against multidrug-resistant *P. aeruginosa* by miss-balancing of oxidation and antioxidation activities interference with the elimination of ROS. The antimicrobial activity of AgNps performed by Lekshmi et al. [49] showed that AgNps possessed maximum antibacterial effect. Results revealed that freshly prepared silver nanoparticles (FGAgNPs) and Gaqu extract had a greater bactericidal effect against all the tested bacterial pathogens except *S. epidermidis* (Table 1). Similarly, calcined silver nanoparticles had a significant antibacterial effect compared to the stored nanoparticles. *Klebsiella pneumoniae* results showed that Gaqu, stored GAgNps at RT and calcined GAgNps at 700°C, showed moderate inhibition (5.66, 5.66, and 5.66 mm). The highest sensitivity was observed in the case of FGAgNps, calcined GAgNps at 300°C, 500°C, and GAgNps stored at 37°C and 4°C (9.66, 9.66, 7.0, 6.65, and 7.33 mm), respectively. The antibacterial activity indicated that FGAgNps showed maximum zone of inhibition (6.33 mm) while Gaqu, stored GAgNps at RT and calcined GAgNps at 300°C, exhibited moderate inhibition (4.0, 4.33, and 5.0 mm) of *Serratia marcescens*. In the case of *Streptococcus pyogenes*, it was observed that Gaqu showed maximum zone of inhibition (7.0 mm), whereas calcined nanoparticles at 300°C showed moderate inhibition (4.33 mm). On the other hand, FGAgNps, stored GAgNps at 4°C, RT, and 37°C and calcined at 500°C and 700°C, showed low sensitivity (1.33, 2.0, 1.66, 2.33, 1.66, and 2.0 mm). FGAgNps, stored GAgNPs at 4°C, calcined GAgNps at 500°C and 700°C, showed the highest inhibition of *Pseudomonas aeruginosa* (8.33, 6.66, 6.33, and 7.66 mm), whereas Gaqu, stored GAgNps at RT and 37°C, showed moderate inhibition (5.66, 4.66, and 4.66 mm). In the case of *Staphylococcus aureus* (a), FGAgNPs, Gaqu, and calcined GAgNPs at 300°C and 500°C had the highest zone of inhibition (11.0, 6.33, 8.66, and 6.66 mm). Gaqu showed maximum inhibition of *Staphylococcus aureus* (b) (5.33 mm) while stored GAgNps at 4°C showed moderate inhibition (4.33 mm), and FGAgNps, calcined GAgNps at 500°C and 700°C, 300°C, stored GAgNps at RT, and Gaqu had the lowest effect. In the case of *Staphylococcus aureus* (c), it was observed that FGAgNps and stored GAgNps at RT and 37°C showed the highest antibacterial effect (7.0, 7.33, and 8.33 mm). On the other hand, stored GAgNps at 4°C and calcined GAgNPs at 300°C had a moderate effect on the growth of *S. aureus* (c) with 5.0 mm and 5.66 mm zone of inhibition. The results revealed that all stored and calcined GAgNPs had the lowest antibacterial effect against *E. coli* (b). In the current research, the

antibacterial activities of Gaqu, FGAgNPs, stored, and calcined GAgNps were evaluated, and the significant antibacterial effect was recorded. It was observed that AgNps showed two types of antibacterial activity: inhibitory action and biocidal action [50]. The following mechanisms may be involved in bactericidal action: (1) production of reactive oxygen species, (2) bacterial protein degradation via sulfhydryl groups, (3) release of silver ions in the cell wall of bacterial cells [51], (4) AgNps hinder the transcription and translational processes of a bacterial cell by damaging the genetic material, and (5) inhibition of metabolic activities [52].

In the current research, the spread plate method, biofilm reduction assay, and cell viability assay supported the findings of the agar well-diffusion method. After agar well-diffusion assay, the antibacterial effect of garlic extract (Gaqu), freshly prepared (FGAgNPs), one month-stored, calcined GAgNPs, and $AgNO_3$ was analyzed on the colonies production via the spread plate method. Results revealed that FGAgNPs significantly reduced the colonies of *S. marcescens*, *S. pyogenes*, *S. aureus* (a), *S. aureus* (b), *S. aureus* (c), *K. pneumoniae*, *P. aeruginosa*, *E. coli* (b), and *S. epidermidis* on agar plates after overnight incubation (Figure 4). Similarly, FGAgNps showed significant biofilm inhibition of all the tested bacterial pathogens compared to calcined GAgNps and stored GAgNps. It was observed that stored GAgNps at 37°C and RT showed biofilm reduction of all the tested pathogens compared to stored GAgNps at 4°C and antibiotics. On the other hand, calcined GAgNps at 700°C had the lowest biofilm inhibition compared to calcined GAgNps of 300°C and 500°C. Du et al. [53] showed that AgNps synthesized by using banana in grams had an antibiofilm effect up to the concentration of 10 µg/mL. Yun'an et al. [54] demonstrated that microbes can be combated with antibiofilm activity with AgNPs. In the case of cell viability assay, we observed that FGAgNps showed the cell proliferation inhibition of all the tested bacterial pathogens. On the other hand, stored GAgNps at RT and 37°C are more effective compared to store GAgNps at 4°C. Similarly, calcined GAgNPs at 300°C and 500°C showed maximum cell proliferation inhibition compared to 700°C calcined GAgNps. Some researchers have suggested that AgNps showed variations in the antibacterial effect against both Gram-negative and Gram-positive bacteria [55]. This could be due to the possible interaction of Gram-negative bacterial membrane with positively charged AgNps and also leads to membrane alteration and increased the permeability of the bacterial membrane which results in cell death [56].

3.3 DPPH radical scavenging assay

The aqueous garlic extract (Gaqu) showed moderate scavenging activity (56.3%) when treated with DPPH solution while GAgNPs showed the highest antioxidant activity (Table 2). It was observed that freshly prepared FGAgNPs showed the highest scavenging activity (84.6%). On the other hand, GAgNPs calcined at 300°C showed 79% scavenging activity compared to the calcined GAgNPs at 500°C and 700°C (76.5% and 73%).

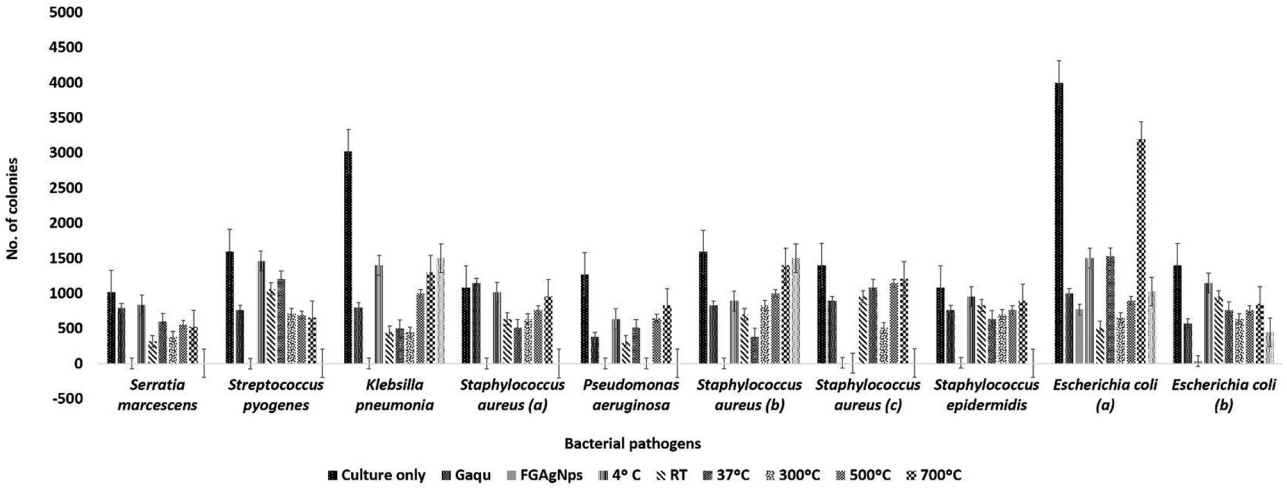

Figure 4: Antibacterial efficacy of green-synthesized silver nanoparticles using *A. sativum* clove extract via the spread plate agar method.

Table 2: *In vitro* biological activity of green-synthesized silver nanoparticles (GAgNPs) and the extract of *Allium sativum* (Gaqu)

Treatments ↓ parameters →	DPPH scavenging potential effect (%)	Iron-chelation effect (% inhibition)	Coagulation time (min:s)	Hemolytic effect (%)	Protein kinase inhibition assay (%)
Gaqu	56.30	11.59	8:50	52	7
FGAgNps	84.6	61.07	24:11	73	14
4°C	29	21	10:56	51	10
RT	48.7	42.40	12:53	56	13
37°C	40	27	22:23	61	11
300°C	79	72.70	31:23	65	12
500°C	76.5	70.00	21:22	64	14
700°C	73	60	18:26	62	0

While stored GAgNPs' (at room temperature) 48.7% scavenge potentially compared to the stored GAgNPs at 37°C and 4°C (40% and 29%). The results reveal that with the increase in calcination temperature, GAgNPs' efficiency decreased. On the other hand, it was observed that calcined GAgNPs and freshly prepared (FGAgNPs) possessed higher antioxidant activity than stored GAgNPs and the aqueous garlic extract (Gaqu). Our results are inconsistent with the findings of Kharat and Mendhulkar [57], who revealed that green-synthesized AgNPs using the aqueous leaf extract of *E. scaber* had strong scavenge DPPH free radicals (85.90%), but it was observed that AgNPs synthesized by using aqueous garlic, green tea, and turmeric extracts showed efficient antioxidant activity compared to the ascorbic acid [58]. Extracts of marine algae *Ecklonia cava* have been used to synthesize AgNPs. Biosynthesized AgNPs showed efficient antioxidant activity determined by (DPPH) scavenging assay. Both the extract and its AgNPs showed 50% scavenging activity at 250 µg/mL [59]. AgNPs synthesized by a green method using 4-*N*-methyl benzoic acid, which is a phenolic derivative isolated from *Memecylon umbellatum* Burm F., had the potential scavenge DPPH radical effect (81.57%) [60].

3.4 Iron-chelating activity

Table 2 results showed that garlic extract (Gaqu) possessed low metal-chelating activity (11.59%) compared to GAgNPs. It was observed that freshly prepared FGAgNPs and GAgNPs calcined at 300°C showed the highest metal-chelating activity (61.07% and 72.70%) and efficiently inhibited the ferrozine–Fe^{2+} complex formation compared to others. On the other hand, GAgNPs stored at room temperature possessed 42.40% metal-chelating potential, which is greater than the stored GAgNPs at 37°C and 4°C. The results reveal that with the increases in the calcination temperature, GAgNPs' efficiency is going to reduce but calcined GAgNPs possess higher metal-chelating potential than the stored GAgNPs. Our results are agreed with the previous studies that AgNPs synthesized by using *Artemisia haussknechtii* leaf aqueous extract showed significant metal-chelating activity (68.93 % ± 2.37) [61]. Silver nanoparticles (AgNPs) synthesized from 4-*N*-methyl benzoic acid, which is a phenolic derivative isolated from *Memecylon umbellatum* Burm F., showed the metal-chelating potential ranging from 21.9% to 82.49% [60]. Liu et al. [62] reported that after the boiling procedure, chelating activities of ferrous ions by garlic aqueous extracts increased about 54.7% do not agree with our results. Edible and nonedible plants contain phenolic compounds having several biological effects including antioxidant activity. Phenolic-rich extracts are of great importance to the pharmaceutical and food industry [63].

3.5 Anticoagulant assay

The results revealed that freshly prepared FGAgNPs, stored, and calcined GAgNPs prolonged the clot formation time more efficiently compared to controls and Gaqu extract (Table 2). The findings showed that the coagulation time of plasma increases with the addition of garlic extract (8 min:50 s) but not significantly compared to the GAgNPs. Negative control has to mean a coagulation time of 5 min:40 s. Our results are consistent with the previous studies of Asha [64]. Certain phytochemical components in the extract are responsible for the increasing prothrombin time [64].

3.6 Hemolytic activity

It was observed that the FGAgNPs showed minimum hemolysis compared to the stored and calcined silver nanoparticles (GAgNPs) and the Gaqu extract (Table 2). We can say that FGAgNPs could be less toxic compared to others. Interesting results were also observed that hemolysis is dose-dependent; with the increase in the dose of GAgNPs and garlic extract, the percentage of hemolysis also increases (Table 2). Our findings are in agreement with other previous studies [65,66]. Raja et al. [65] studied the *in vitro* hemolytic activity of AgNPs synthesized by using *Catharanthus roseus* and showed that AgNPs were found to be nontoxic at the lowest concentration (1–5 µg/mL) and toxic at the highest concentration (15–50 µg/mL). So, we can say that increased concentration would be toxic. In another study, it was found that various solvent fractions of *Croton bonplandianum* showed hemolytic activity, which depends on the dose of extract. Increasing the dose of extract also increases the percentage of hemolysis [66]. Saponins present in plants increase the permeability of the membrane and cause hemolysis. These are reflected as potential adjuvants. It was recorded that the hemolytic effect of any compounds/molecules depends upon numerous factors such as temperature, incubating time, side chain which consists of saponin and membrane composition [67,68].

3.7 Antidiabetic activity

It was found interesting that freshly prepared FGAgNPs showed maximum inhibition (75.55%) at 50 µg/mL, and the IC_{50} value of FGAgNPs was calculated as 2.38 µg/mL as shown in Table 3. GAgNPs (stored at room temperature and at 4°C in the fridge) showed moderate amylase inhibition in contrast with GAgNPs stored at 37°C in an incubator for one month. The IC_{50} value of GAgNPs (stored at 4°C in the fridge, at room temperature, and 37°C in an incubator) was recorded as 55.68, 31.96, and 7.19 µg/mL, respectively. The calcined GAgNps at 700°C efficiently inhibit amylase activity compared to GAgNPs calcined at 300°C and 500°C. The IC_{50} value for calcined GAgNps at 300°C, 500°C, and 700°C was calculated as 31.02, 22.43, and 6.86 µg/mL, respectively. Results also showed that the garlic extract (Gaqu) possesses the least amylase-inhibition capacity possessing an IC_{50} value of 97.79 µg/mL. The undertaken study revealed that the efficiency of one month-stored and calcined AgNPs increased with the increase in temperature. It has also been observed that with the increase in the concentration of AgNPs either stored or calcined, the activity of α-amylase was more efficiently inhibited. Vishnu and Murugesan [69] revealed similar results by using silver nanoparticles synthesized from *Halymenia poryphyroides* that showed momentous *in vitro* antidiabetes efficiency in a dose-dependent manner with an increase in percentage alpha-amylase inhibitory activity. The garlic GAgNPs have the potential to inhibit alpha-amylase activity. The garlic AgNPs minimized the amylase level, which is responsible for the hydrolysis of complex carbohydrates into simpler carbohydrates to enhance the consumption of glucose. Similar results were reported by Rajaram et al. [70], Abideen and Sankar [71], and Sengottaiyan et al. [72]. The inhibition of amylase enzyme is specifically involved in the treatment of insulin-independent diabetes as it slows down the release of glucose in the blood. The results point out that alpha-amylase was considerably inhibited in a dose-dependent manner following incubation at different concentrations of silver nanoparticles. Our results are agreed with the previous studies [70,73]. According to various *in vivo* studies, for diabetes care, alpha-amylase inhibition is supposed to be one of the most operative methods [74,75].

Table 3: Antidiabetic effect of green-synthesized silver nanoparticles (GAgNPs) and the extract of *Allium sativum* (Gaqu)

Treatments ↓ concentrations →	% Inhibition (1,000 µg/mL)			IC_{50} (µg/mL)
	10 µL	30 µL	50 µL	
G.aqu	36.21	39.22	42.44	97.79
FGAgNPs	54.35	66.15	75.55	2.38
4°C	41.21	44.53	49.09	55.68
RT	44.50	47.70	56.11	31.96
37°C	51.12	55.61	62.17	7.19
300°C	32.95	50.14	64.48	31.02
500°C	40.12	55.16	73.85	22.43
700°C	51.47	64.75	75.49	6.86

3.8 Brine shrimp toxicity assay

A huge number of extracts of medicinal plants were screened for the drug formulation, and *in vitro* toxicological procedure, i.e., brine shrimp (*Artemia salina*) assay was used [76,77]. In the present research, it was observed that FGAgNPs showed a stronger toxic effect and caused the high mortality of larvae (70%) compared

Table 4: Brine shrimp toxicity assay of green-synthesized silver nanoparticles (GAgNPs) and the extract of *Allium sativum* (Gaqu).

Treatments↓ concentrations →	Number of brine shrimp killed after 24 h			
	25 µg/mL	50 µg/mL	100 µg/mL	200 µg/mL
FGAgNps	10 ± 0.0	30 ± 0.0	60 ± 0.0	70 ± 0.0
4°C	10 ± 0.0	30 ± 0.0	45 ± 0.0	50 ± 0.0
RT	15 ± 0.0	35 ± 0.0	46 ± 0.0	65 ± 0.0
37°C	10 ± 0.0	35 ± 0.0	52 ± 0.0	64 ± 0.0
300°C	15 ± 0.0	25 ± 0.0	45 ± 0.0	55 ± 0.0
500°C	10 ± 0.0	25 ± 0.0	40 ± 0.0	60 ± 0.0
700°C	10 ± 0.0	10 ± 0.0	30 ± 0.0	30 ± 0.0
Doxorubicin	0 ± 0.0	40 ± 0.0	60 ± 0.0	80 ± 0.0

to other GAgNPs at 200 µg/mL (Table 4). Similarly, GAgNPs stored at room temperature at 37°C also showed the maximum mortality (65% and 64%) at 200 µg/mL compared to stored 4°C, but it was less toxic than FGAgNPs. GAgNPs calcined at 700°C were less toxic toward the brine shrimp (30%) at 200 µg/mL compared to the calcined GAgNPs at 500°C and 300°C. It was observed that the cytotoxic effect was also dose-dependent, and the mortality rate was increased with increase in concentration (Table 4). Hence, the results disclosed that as the concentration increases, the lethality rate also increases. Our results are in agreement with AshaRani et al. [78]. Zubia et al. [79] reported that the extract of *Asparagopsis armata* and *Laurencia obtuse* have a strong cytotoxic effect against cancer cell lines. Doxorubicin (positive control) indicates 80% mortality at 200 µg/mL.

3.9 Protein kinase inhibition assay

FGAgNPs have the highest zone of inhibition (18.0 ± 0.0 mm) compared to all GAgNPs at 50 µg/disc (Table 2) compared to all treatments. Among the stored GAgNps, room temperature-stored GAgNPs showed the highest zone of inhibition (13 ± 0.0 mm), and the least was shown by GAgNPs stored at 4°C (10.0 ± 0.0 mm). Similarly, the calcined GAgNPs at 500°C and 300°C exhibited 14.0 ± 0.0 mm and 12.0 ± 0.0 mm zone of inhibition, respectively. On the other hand, GAgNPs calcined at 700°C did not exhibit. Surfactin was used as a positive control which showed 22.0 ± 0.0 mm zone of inhibition. The results depict that GAgNPs can hinder protein kinase activity. The results of the present study revealed that phytochemicals present in the garlic extract could serve as protein kinase inhibitors. Protein kinase enzymes are involved in different biological activities that include cell differentiation, cell proliferation, apoptosis, and metabolism by causing phosphorylation of proteins at tyrosine and serine/threonine residues [15,47]. The result of genetic variations causes protein kinases to deregulate phosphorylation of protein at tyrosine and serine/threonine residues, which cause cancer. In this regard, the preferred target for cancer treatment is protein kinase inhibition [80].

4 Conclusion

Silver nanoparticles have been successfully synthesized using *Allium sativum* bulb extract. The synthesis and stability of GAgNPs are found to be efficient. The freshly prepared silver nanoparticles (FGAgNPs) are found to have a significant antibacterial, antidiabetic, anticoagulant, and antioxidant effects. Due to these properties, GAgNPs are efficiently used in the field of medicine to prevent both infectious and noninfectious diseases.

Acknowledgments: The authors are grateful to the Department of Physics, the University of Azad Jammu and Kashmir, Muzaffarabad, for providing research facilities. The authors also extend their appreciation to the researchers supporting project number RSP-2020/190/, King Saud University, Riyadh, Saudia Arabia.

References

[1] Chashoo I, Kumar D, Bhat Z, Khan N, Kumar V, Nowshehri JA. Antimicrobial studies of *Sambucus wightiana* Wall. ex. Wight & Arn. J Pharm Res. 2012;5:2467–8.

[2] Krishnaraj C, Jagan EG, Rajasekar S, Selvakumar P, Kalaichelvan PT, Mohan N. Synthesis of silver nanoparticles using Acalyphaindica leaf extracts and its antibacterial activity against water-borne pathogens. Colloids Surf B. 2010, 1;76(1):50–60.
[3] Baker. S, Rakshith D, Kavitha KS, Santosh P, Kavitha HU, Rao Y, et al. Plants: emerging as nanofactories towards facile route in synthesis. BioImpacts Nanopart. 2013;3(3):111–7.
[4] Makarov VV, Love AJ, Sinitsyna OV, Makarova SS, Yaminsky IV, Taliansky ME, et al. Green nanotechnologies: synthesis of metal nanoparticles using plants. Acta Nat. 2014;6:1–20.
[5] Oh KH, Soshnikova V, Markus J, Kim YJ, Lee SC, Singh P, et al. Biosynthesized gold and silver nanoparticles by aqueous fruit extract of Chaenomeles sinensis and screening of their biomedical activities. Artif Cells Nanomed Biotechnol. 2018;46(3):599–606.
[6] Mori Y, Ono T, Miyahira Y, Nguyen VQ, Matsui T, Ishihara M. Antiviral activity of silver nanoparticle/chitosan composites against H1N1 influenza A virus. Nanoscale Res Lettt. 2013;8(1):93.
[7] Wong KK, Cheung SO, Huang L, Niu J, Tao C, Ho CM, et al. Further evidence of the anti-inflammatory effects of silver nanoparticles. ChemMedChem. 2009;4(7):1129–35.
[8] Johnson P, Krishnan V, Loganathan C, Govindhan K, Raji V, Sakayanathan P, et al. Rapid biosynthesis of Bauhinia variegata flower extract-mediated silver nanoparticles: an effective antioxidant scavenger and α-amylase inhibitor. Artif Cells Nanomed Biotechnol. 2018;46(7):1488–94.
[9] Dehghanizade S, Arasteh J, Mirzaie A. Green synthesis of silver nanoparticles using *Anthemis atropatana* extract: characterization and *in vitro* biological activities. Artif Cells Nanomed Biotechnol. 2018;46(1):160–8.
[10] Moteriya P, Chanda S. Synthesis and characterization of silver nanoparticles using *Caesalpinia pulcherrima* flower extract and assessment of their *in vitro* antimicrobial, antioxidant, cytotoxic, and genotoxic activities. Artif Cells Nanomed Biotechnol. 2017;45(8):1556–67.
[11] Fouad H, Hongjie L, Hosni D, Wei J, Abbas G, Ga'al H, et al. Controlling *Aedes albopictus* and *Culex pipiens* pallens using silver nanoparticles synthesized from aqueous extract of *Cassia fistula* fruit pulp and its mode of action. Artif Cells Nanomed Biotechnol. 2018;46(3):558–67.
[12] Singh H, Du J, Singh P, Yi TH. Ecofriendly synthesis of silver and gold nanoparticles by *Euphrasia. officinalis* leaf extract and its biomedical applications. Artif Cells Nanomed Biotechnol. 2018;46(6):1163–70.
[13] Huo Y, Singh P, Kim YJ, Soshnikova V, Kang J, Markus J, et al. Biological synthesis of gold and silver chloride nanoparticles by Glycyrrhiza uralensis and *in vitro* applications. Artif Cells Nanomed Biotechnol. 2018;46(2):303–12.
[14] Vijayan R, Joseph S, Mathew B. Indigofera tinctoria leaf extract mediated green synthesis of silver and gold nanoparticles and assessment of their anticancer, antimicrobial, antioxidant and catalytic properties. Artif Cells Nanomed Biotechnol. 2018;46(4):861–71.
[15] Zia G, Sadia H, Nazir S, Ejaz K, Ali S, Iqbal T, et al. *In vitro* studies on cytotoxic, DNA protecting, antibiofilm and antibacterial effects of Biogenic silver nanoparticles prepared with Bergenia ciliata rhizome extract. Curr Pharm Biotechnol. 2018;19(1):68–78.
[16] Pavithra BV, Ragavendran C, Murµgan N, Natarajan D. Ipomoea batatas (Convolvulaceae)-mediated synthesis of silver nanoparticles for controlling mosquito vectors of Aedes albopictus, Anopheles stephensi, and Culex quinquefasciatus (Diptera: Culicidae). Artif Cells Nanomed Biotechnol. 2017;45(8):1568–80.
[17] Lateef A, Folarin BI, Oladejo SM, Akinola PO, Beukes LS, Gueguim-Kana EB. Characterization, antimicrobial, antioxidant, and anticoagulant activities of silver nanoparticles synthesized from *Petiveria alliacea* L. leaf extract. Prep Biochem Biotechnol. 2018;48(7):646–52.
[18] Singh TU, Kumar D, Tandan SK, Mishra SK. Inhibitory effect of essential oils of *Allium sativum* and *Piper longum* on spontaneous muscular activity of liver fluke, *Fasciola gigantica*. Exp Parasitol. 2009;123(4):302–8.
[19] Tattelman E. Health effects of garlic. Am Fam Physician. 2005;72(1):103–6.
[20] Awan UA, Ali S, Shahnawaz AM, Shafique I, Zafar A, Rauf Khan MA, et al. Biological activities of Allium sativum and Zingiber officinale extracts on clinically important bacterial pathogens, their phytochemical and FT-IR spectroscopic analysis. Pak J Pharm Sci. 2017;30(3):729–45.
[21] Hosseini A, Hosseinzadeh H. A review on the effects of Allium sativum (Garlic) in metabolic syndrome. J Endocrinolol Invest. 2015;38(11):1147–57.
[22] Charu. K, Yogita S, Sonali S. Neutraceutical potential of organosulphur compounds in fresh garlic and garlic preparations. IJPBS. 2014;5(1):112–26.
[23] Liu CT, Wong PL, Lii CK, Hse H, Sheen LY. Antidiabetic effect of garlic oil but not diallyl disulfide in rats with streptozotocin-induced diabetes. FCT. 2006;44(8):1377–84.
[24] Hafeez K, Andleeb S, Ghousa T, Mustafa R, Naseer A, Shafique I, et al. Phytochemical screening, alpha gluosidase inhibition, antibacterial and antioxidant potential of Ajµga bracteosa extracts. Curr Pharm Biotechnol. 2017;18(4):336–42.
[25] Rios J, Recio M, Villar A. Screening methods for natural products with antimicrobial activity: a review of the literature. J Ethnopharmacol. 1988;23(2–3):127–49.
[26] Seeley HW, Vandemark PJ, Lee JJ. Microbes in action, a labortary manual of microbiology, 4th edn. New York: W. H. Freeman and Co.; 2001. p. 57–130.
[27] Hammer KA, Carson CF, Riley TV. Antimicrobial activity of essential oils and other plant extracts. J Appl Microbiol. 1999;86(6):985–90.
[28] Hartman D. Perfecting your spread plate technique. JMBE. 2011;12(2):204.
[29] Raja AF, Ali F, Khan IA, Shawl AS, Arora DS, Shah BA, et al. Anti-staphylococcal and biofilm inhibitory activities of acetyl11-keto-β-boswellic acid from Boswellia serrate. BMC Microbiol. 2011;11:1–9.
[30] Gerlier D, Thomasset N. Use of MTT colorimetric assay to measure cell activation. J Immunol Methods. 1986;94(1–2):57–63.
[31] Dandjesso C, Klotoa JR, Doµgnon TV, Sègbo J, Atègbo JM, Gbaguidi F, et al. Phytochemistry and hemostatic properties of some medicinal plants sold as anti-hemorrhagic in Cotonou markets (Benin). Ind J Sci Technol. 2012;5(8):3105–9.
[32] Yang ZG, Sun HX, Fang WH. Haemolytic activities and adjuvant effect of Astragalus membranaceus saponins (AMS) on the

immune responses to ovalbumin in mice. Vaccine. 2005;23(44):5196–203.
[33] Brand-Williams W, Cuvelier ME, Berset CLWT. Use of a free radical method to evaluate antioxidant activity. LWT-Food Sci Technol. 1995;28(1):25–30.
[34] Dinis TCP, Madeira VMC, Almeida MLM. Action of phenolic derivates (acetoaminophen, salycilate and 5-aminosalycilate) as inhibitors of membrane lipid peroxidation and as peroxyl radical scavengers. Arch Biochem Biophys. 1994;315:161–9.
[35] Malik CP, Singh MB. A text manual plant enzymology and histoenzymology. New Delhi: NavinShandara; 1980. p. 66–71.
[36] Fatima H, Khan K, Zia M, Ur-Rehman T, Mirza B, Haq IU. Extraction optimization of medicinally important metabolites from Daturainnoxia Mill: an *in vitro* biological and phytochemical investigation. BMC Complement Altern Med. 2015;15(1):376–82.
[37] Bibi Y, Nisa S, Chaudhary FM, Zia M. Antibacterial activity of some selected medicinal plants of Pakistan. BMC Complement Altern Med. 2011;11(1):52–56.
[38] Shankar SS, Rai A, Ahmad A, Sastrya M. Rapid synthesis of Au, Ag, and bimetallic Au core–Ag shell nanoparticles using Neem (*Azadirachta indica*) leaf broth. J Colloid Interface Sci. 2004;275(2):496–502.
[39] Rajeshkumar S. Synthesis of silver nanoparticles using fresh bark of Pongamia pinnata and characterization of its antibacterial activity against gram positive and gram negative pathogens. Resource-Efficient Technol. 2016;2(1):30–5.
[40] Donda MR, Kudle KR, Alwala J, Miryala A, Sreedhar B, Rudra MP. Synthesis of silver nanoparticles using extracts of Securinegaleucopyrus and evaluation of its antibacterial activity. IJCST. 2013;7:1–8.
[41] Sharma S, Kumar S, Bulchandini B, Taneja S, Banyal S. Green synthesis of silver nanoparticles and their antimicrobial activity against gram-positive and gram negative bacteria. IJBB. 2013;4(7):711–4.
[42] Li S, Shen Y, Xie A, Yu X, Qiu L, Zhang L, et al. Green synthesis of silver nanoparticles using *Capsicum annuum* L. extract. Green Chem. 2007;9(8):852–8.
[43] Pohlit AM, Rezende AR, Baldin ELL, Lopes NP, de Andrade Neto VF. Plant extracts, isolated phytochemicals, and plant-derived agents which are lethal to arthropod vectors of human tropical diseases – a review. Planta Med. 2011;77(6):618–30.
[44] Link S, Sayed MA. Optical properties and ultrafast dynamics of metallic nanocrystals. Ann Rev Phys Chem. 2003;54:331–66.
[45] El-Refai AA, Ghoniem GA, El-Khateeb AY, Hassaan MM. Eco-friendly synthesis of metal nanoparticles using ginger and garlic extracts as biocompatible novel antioxidant and antimicrobial agents. J Nanostruct Chem. 2018;8(1):71–81.
[46] Otunola GA, Afolayan AJ, Ajayi EO, Odeyemi SW. Characterization, antibacterial and antioxidant properties of silve nanoparticles synthesized from aqueous extracts of *Allium sativum, Zingiber officinale*, and *Capsicum frutescens*. Pharmacogn Mag. 2017;13(2):201.
[47] Ejaz K, Sadia H, Zia G, Nazir S, Raza A, Ali S, et al. Biofilm reduction, cell proliferation, anthelmintic and cytotoxicity effect of green synthesised silver nanoparticle using *Artemisia vulgaris* extract. IET Nanobiotechnol. 2017;12(1):71–7.
[48] Liao S, Zhang Y, Pan X, Zhu F, Jiang C, Liu Q, et al. Antibacterial activity and mechanism of silver nanoparticles against multidrug-resistant *Pseudomonas aeruginosa*. Int J Nanomed. 2019;14:14–69.
[49] Lekshmi NC, Sumi SB, Viveka S, Jeeva S, Brindha JR. Antibacterial activity of nanoparticles from *Allium* sp. Microbiol Biotechnol Res. 2012;2(2):115–9.
[50] Perni S, Hakala P, Prokopovich P. Biogenic synthesis of antimicrobial silver nanoparticles capped with L-cysteine. Colloids Surf Physicochem Eng Asp. 2014;460:219–24.
[51] Patil RS, Kokata MR, Kolekar SS. Bioinspired synthesis of highly stabilized silver nanoparticles using ocimum tenuiflorum leaf extract and their antibacterial activity. Spectrochim Acta Part A Mol Biol Mol Spectrosc. 2012;91:234–8.
[52] Ahmed S, Saifullah A, Ahmad M, Swami BL, Ikram S. Green synthesis of silver nanoparticles using *Azadirachta indica* aqueous leaf extract. J Radiat Res Appl Sci. 2016;9(1):1–7.
[53] Du J, Singh H, Yi TH. Antibacterial, anti-biofilm and anticancer potentials of green synthesized silver nanoparticles using benzoin gum (*Styrax benzoin*) extract. Bioproc Biosyst Eng. 2016;39(12):1923–31.
[54] Yun'an Q, Cheng L, Li R, Liu G, Zhang Y, Tang X, et al. Potential antibacterial mechanism of silver nanoparticles and the optimization of orthopedic implants by advanced modification technologies. Int J Nanomed. 2018;13:3311.
[55] Sadeghi B, Gholamhoseinpoor F. A study on the stability and green synthesis of silver nanoparticles using Ziziphora tenuior (Zt) extract at room temperature. Spectrochim Acta Part A Mol Biomol Spectrosc. 2015;134:310–5.
[56] Chanda S. Silver nanoparticles: a new generation of antimicrobials to combat microbial pathogens – a review. Formatex. 2013;1314–23.
[57] Kharat SN, Mendhulkar VD. Synthesis, characterization and studies on antioxidant activity of silver nanoparticles using Elephantopus scaber leaf extract. Mater Sci Eng C. 2016;62:719–24.
[58] Selvan DA, Mahendiran D, Kumar RS, Rahiman AK. Garlic, green tea and turmeric extracts-mediated green synthesis of silver nanoparticles: phytochemical, antioxidant and *in vitro* cytotoxicity studies. J Photochem Photobiol B. 2018;180:243–52.
[59] Venkatesan J, Kim SK, Shim M. Antimicrobial, antioxidant, and anticancer activities of biosynthesized silver nanoparticles using marine algae *Ecklonia cava*. Nanomater. 2016;6(12):235.
[60] AlSalhi MS, Elangovan K, Ranjitsingh AJA, Murali P, Devanesan S. Synthesis of silver nanoparticles using plant derived 4-*N*-methyl benzoic acid and evaluation of antimicrobial, antioxidant and antitumor activity. Saudi J Biol Sci. 2019;26(5):970–78.
[61] Alavi M, Karimi N. Characterization, antibacterial, total antioxidant, scavenging, reducing power and ion chelating activities of green synthesized silver, copper and titanium dioxide nanoparticles using Artemisia haussknechtii leaf extract. Artif Cells Nanomed Biotechnol. 2018;46(8):2066–81.
[62] Liu C, Yang X, Yao Y, Huang W, Sun W, Ma Y. Determination of antioxidant activity in garlic (*Allium sativum*) extracts subjected to boiling process *in vitro*. J Food Nutr Res. 2014;2(7):383–7.
[63] Kähkönen MP, Hopia AI, Vuorela HJ, Rauha JP, Pihlaja K, Kujala TS, et al. Antioxidant activity of plant extracts

containing phenolic compounds. J Agric Food Chem. 1999;47(10):3954–62.
[64] Asha S. *In vitro* anticoagulant activity of Nelumbo nucifera leaf extracts on normal healthy blood plasma. IJGP. 2017;11:03.
[65] Raja A, Salique SM, Gajalakshmi P, James A. Antibacterial and hemolytic activity of green silver nanoparticles from Catharanthus roseus. IJPSN. 2016;9(1):3112–7.
[66] Ghosh T, Biswas MK, Roy P. An evaluation of antibacterial potential of medicinal plant Croton bonplandianum against some pathogen isolated from complicated urinary tract infections (UTI): alternative approaches of conventional treatment. World J Pharm Res. 2018;7(9):1323–42.
[67] Noudeh GD, Sharififar F, Behravan E, Mohajeri E, Alinia V. Medicinal plants as surface activity modifiers. JMPR. 2011;5(22):5378–83.
[68] Urbanska N, Nartowska J, Skorupska A, Ruszkowski D, Giebultowicz J, Olszowska O. Determination and haemolytic activity of saponins in hairy root culture of *Platycodon grandiflorum* A. DC. Herba Pol. 2009;3(55):103–8.
[69] Vishnu K, Murµgesan M. S. Biogenic silver nanoparticles by Halymeniaporyphyroides and its *in vitro* anti-diabetic efficacy. J Chem Pharm Res. 2013;5(12):1001–8.
[70] Rajaram K, Aiswarya DC, Sureshkumar P. Green synthesis of silver nanoparticle using *Tephrosiatinctoria* and its antidiabetic activity. Mater Lett. 2015;138:251–4.
[71] Abideen S, Sankar M. *In vitro* screening of antidiabetic and antimicrobial activity against green synthesized $AgNO_3$ using seaweeds. J Nanomed Nanotechnol. 2015;10:2157–7439.
[72] Sengottaiyan A, Aravinthan A, Sudhakar C, Selvam K, Srinivasan P, Govarthanan M, et al. Synthesis and characterization of Solanumnigrum mediated silver nanoparticles and its protective effect on alloxan-induced diabetic rats. JNC. 2016;6(1):41–8.
[73] Sivaranjani K, Meenakshisundaram M. Biological synthesis of silver nanoparticles using Ocimum basillicum leaf extract and their antimicrobial activity. Int Res J Pharm. 2013;4(1):225–9.
[74] Balan K, Perumal P, Sundarabaalaji N, Palvannan T. Synthesis, molecular modeling and biological evaluation of novel 2-allyl amino 4-methyl sulfanyl butyric acid as α-amylase and α-glucosidase inhibitor. J Mol Struct. 2015;1081:62–8.
[75] Hamid HA, Yusoff MM, Liu M, Karim MR. α-Glucosidase and α-amylase inhibitory constituents of Tinosporacrispa: Isolation and chemical profile confirmation by ultra-high performance liquid chromatography-quadrupole time-of-flight/mass spectrometry. J Funct Foods. 2015;16:74–80.
[76] Ramazani A, Zakeri S, Sardari S, Khodakarim N, Djadidt ND. *In vitro* and *in vivo* anti-malarial activity of Boerhaviaelegans and Solanumsurattense. Malar J. 2010;9(1):124–8.
[77] Sangian H, Faramarzi H, Yazdinezhad A, Mousavi SJ, Zamani Z, Noubarani M, et al. Antiplasmodial activity of ethanolic extracts of some selected medicinal plants from the northwest of Iran. Parasitol Res. 2013;112(11):3697–701.
[78] AshaRani PV, Low KahMun G, Hande MP, Valiyaveettil S. Cytotoxicity and genotoxicity of silver nanoparticles in human cells. ACS Nano. 2008;3(2):279–90.
[79] Zubia M, Fabre MS, Kerjean V, Deslandes E. Antioxidant and cytotoxic activities of some red algae (Rhodophyta) from Brittany coasts (France). Bot Mar. 2009;52(3):268–77.
[80] Yao G, Sebisubi FM, Voo LYC, Ho CC, Tan GT, Chang LC. Citrinin derivatives from the soil filamentous fungus Penicillium sp. H9318. J Braz Chem Soc. 2011;22(6):1125–9.